JOURNAL OF MOLECULAR SPECTROSCOPY 158, 409–422 (1993)

The Far-Infrared Fourier Transform Spectrum of H_2Se

IGOR N. KOZIN, STEFAN KLEE, AND PER JENSEN,

Physikalisch-Chemisches Institut, Justus-Liebig-Universität Heinrich-Buff-Ring 58, W-6300 Giessen, Germany

OLEG L. POLYANSKY

Applied Physics Institute, Russian Academy of Science, Uljanov Street 46, 630 000 Nizhnii Novgorod, Russia

AND

IGOR M. PAVLICHENKOV

Russian National Research Center "Kurchatov Institute," 123182 Moscow, Russia

In the present work, we study the spectrum of the H_2Se molecule in the far-infrared region. This work is a continuation of our experimental investigation of the anomalous "fourfold clustering effect" exhibited by the rotational energy levels in the vibrational ground state of H_2Se. The spectrum in the region 30–360 cm^{-1} was measured with a Bruker IFS 120 HR interferometer attached to a 3-m-long cell. In order to observe transitions involving high J and K_a quantum numbers the cell was heated to 90°C. About 2500 lines were identified and fitted using a modified Watson Hamiltonian. Improved sets of rotational and centrifugal distortion constants for all six selenium isotopomers were obtained. It is shown that the fourfold clustering of rotational levels, as well as the observed linestrength distortions, can be explained in terms of localized wavefunctions.

INTRODUCTION

The anomalous behavior of the ground state rotational levels in H_2Se has been the subject of considerable experimental and theoretical interest. In recent MW investigations (*1–3*), where primarily Q-type transitions were measured, it was observed that with increasing J, the rotational energy levels form fourfold clusters. These clusters first occur at the top of each J-multiplet at $J_{CR} = 12$. The MW measurements allow a precise determination of the splittings between the individual cluster components for J up to 23. However, there was no experimental information about the absolute energy position of these highly excited rotational states. In order to obtain this information, we have studied the part of the H_2Se ground state rotational spectrum which falls in the FIR region (*4*).

The spectrum was measured in the region 30–360 cm^{-1} with a Bruker IFS 120 HR interferometer attached to a 3-m-long cell. The main objective of the experimental work was the observation of transitions involving high values of J and K_a. Toward this end, the spectrum was recorded with a sample temperature of 90°C, as well as at room temperature. As a result of this investigation about 2500 lines were identified and fitted to a modified Watson Hamiltonian. Improved sets of rotational and centrifugal distortion constants for all six isotopic species of selenium were obtained.

0022-2852/93 $5.00

The highly precise experimental data from the present work cover the rotational energy levels up to $J = 23$. That gave us the opportunity to analyze wavefunctions of highly excited rotational states and make reasonable interpolations up to $J = 35$, where the rotational Hamiltonian starts to be divergent. The analysis has shown that the rotational wavefunctions are strongly localized for the quantum states with fourfold degeneracy. As a result of this effect, transitions involving these states show linestrength distortion. Under the assumption that the rotational states are localized, simple analytical expressions for the rotational wavefunctions have been obtained. This analysis has led to approximate expressions for the linestrength which explain the intensity anomalies observed experimentally.

EXPERIMENT AND DATA ANALYSIS

As mentioned above, the H_2Se FIR spectra were recorded in the region 30–360 cm^{-1} using a Bruker IFS 120 HR interferometer. The absorption path length was 3 m. The spectrum was recorded at high (6 mbar) and low pressure (0.3 mbar). The interferometer was equipped with a mercury lamp as radiation source, coated Mylar of different thickness as beamsplitters, and a silicon bolometer operating at 4.2 K as detector. Spectra were taken at an unapodized resolution of 0.0019 cm^{-1}. The spectrometer was calibrated by means of standard water lines (*5*). About 200 single scans were coadded to yield the final spectrum. The sample pressure of about 6 mbar was sufficiently high that the molecular linewidth (originating in the combined effect of Doppler and pressure broadening) was wider than the instrumental lineshape. However, to resolve the frequent dense line structures like that presented in Fig. 1 (right), the lower pressure of about 0.3 mbar was used. The left group of six lines in Fig. 1 corresponds to the same rotational transition of six selenium isotopomers present in natural abundance in the H_2Se sample. As already mentioned, the H_2Se spectrum was recorded with the cell heated to 90°C to facilitate the observation of transitions involving high values of J and K_a.

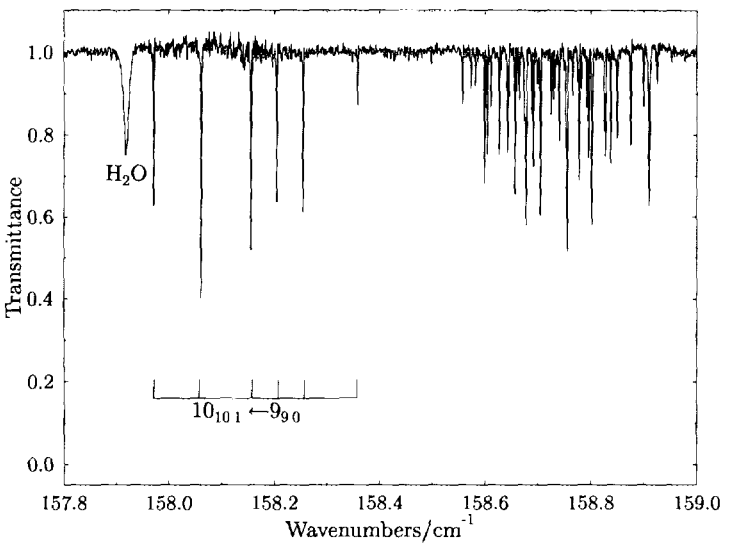

FIG. 1 A. section of the FIR H_2Se absorption spectrum recorded at a pressure of 0.3 mbar.

For line identification the rotational constants of Refs. (*1, 2*) were used. These constants were obtained from a combined fit of the MW data (*1, 2, 6, 7*) and the ground state combination differences given by Refs. (*8, 9*), and so the accuracy of the line frequency prediction was expected to be good enough for line identification. However, due to the presence of dense line groups it was difficult (or impossible) to identify most of the lines belonging to these groups without knowledge of their intensities. Consequently, it proved necessary to make a total prediction list containing not only line positions, but also the intensities of the H_2Se transitions as well as of some impurities such as H_2O and H_2S. To simplify the identification procedure a program was written to process the prediction-list file and the experimental peaklist file consisting of observed line positions and transmittance values. The program chooses line after line in an experimental peaklist file and allows interactively the selection of the most appropriate assignment for the current line from the predicted peaklist file. The chosen assignment can then be automatically entered into the experimental peaklist file, and when all assignments have been chosen, this file may serve as input for the least squares fitting of molecular parameters.

It is known that if the instrumental linewidth is smaller than the molecular linewidth, one can predict the transmittance value with high accuracy, the line intensity being known. That exactly was the case when the pressure in the cell exceeded 5 mbar. Therefore, the prediction of transmittance values and the direct comparison with observed values was possible when the high-pressure spectrum was used. For the low-pressure spectrum, in which the molecular linewidth is less than the width of the instrumental lineshape, a calculation of the expected transmittance is possible (*10*) but requires more sophisticated computations. In this latter case the relative comparison was used.

One of the advantages of the semi-automatic assignment program described above is that the resulting files are almost ready to be used as input for a least-squares fit program. By performing the fitting procedure, new sets of constants are obtained which in turn yield a new predicted peaklist file, and this file can be used for further assignments. The assignment of the spectra was completed after five iterative cycles. As a result about 2500 lines were identified with $J_{max} = 23$, $(K_a)_{max} = 20$.

A modified Watson Hamiltonian (*1*) was used to fit the data:

$$
\begin{aligned}
H = {} & (B + C)/2\hat{J}^2 + (A - (B + C)/2)\hat{J}_z^2 - D_J\hat{J}^4 - D_{JK}\hat{J}^2\hat{J}_z^2 - D_K\hat{J}_z^4 + H_J\hat{J}^6 \\
& + H_{JK}\hat{J}^4\hat{J}_z^2 + H_{KJ}\hat{J}^2\hat{J}_z^4 + H_K\hat{J}_z^6 + c_{40}(\hat{J}^2 - \hat{J}_z^2)^4 + c_{31}(\hat{J}^2 - \hat{J}_z^2)^3\hat{J}_z^2 \\
& + c_{22}(\hat{J}^2 - \hat{J}_z^2)^2\hat{J}_z^4 + c_{13}(\hat{J}^2 - \hat{J}_z^2)\hat{J}_z^6 + c_{04}\hat{J}_z^8 + c_{50}(\hat{J}^2 - \hat{J}_z^2)^5 \\
& + c_{41}(\hat{J}^2 - \hat{J}_z^2)^4\hat{J}_z^2 + c_{32}(\hat{J}^2 - \hat{J}_z^2)^3\hat{J}_z^4 + c_{23}(\hat{J}^2 - \hat{J}_z^2)^2\hat{J}_z^6 \\
& + c_{14}(\hat{J}^2 - \hat{J}_z^2)\hat{J}_z^8 + c_{05}\hat{J}_z^{10} + c_{60}(\hat{J}^2 - \hat{J}_z^2)^6 + c_{51}(\hat{J}^2 - \hat{J}_z^2)^5\hat{J}_z^2 \\
& + c_{42}(\hat{J}^2 - \hat{J}_z^2)^4\hat{J}_z^4 + c_{33}(\hat{J}^2 - \hat{J}_z^2)^3\hat{J}_z^6 + c_{24}(\hat{J}^2 - \hat{J}_z^2)^2\hat{J}_z^8 \\
& + c_{15}(\hat{J}^2 - \hat{J}_z^2)\hat{J}_z^{10} + c_{06}\hat{J}_z^{12} + c_{07}\hat{J}_z^{14} + 1/2[\{(B - C)/4 - d_J\hat{J}^2 - d_K\hat{J}_z^2 \\
& + h_J\hat{J}^4 + h_{JK}\hat{J}^2\hat{J}_z^2 + h_K\hat{J}_z^4 + b_{30}(\hat{J}^2 - \hat{J}_z^2)^3 + b_{21}(\hat{J}^2 - \hat{J}_z^2)^2\hat{J}_z^2 \\
& + b_{12}(\hat{J}^2 - \hat{J}_z^2)\hat{J}_z^4 + b_{03}\hat{J}_z^6 + b_{40}(\hat{J}^2 - \hat{J}_z^2)^4 + b_{31}(\hat{J}^2 - \hat{J}_z^2)^3\hat{J}_z^2
\end{aligned}
$$

$$+ b_{22}(\hat{J}^2 - \hat{J}_z^2)^2\hat{J}_z^4 + b_{13}(\hat{J}^2 - \hat{J}_z^2)\hat{J}_z^6 + b_{04}\hat{J}_z^8 + b_{50}(\hat{J}^2 - \hat{J}_z^2)^5$$
$$+ b_{41}(\hat{J}^2 - \hat{J}_z^2)^4\hat{J}_z^2 + b_{32}(\hat{J}^2 - \hat{J}_z^2)^3\hat{J}_z^4 + b_{23}(\hat{J}^2 - \hat{J}_z^2)^2\hat{J}_z^6$$
$$+ b_{14}(\hat{J}^2 - \hat{J}_z^2)\hat{J}_z^8 + b_{05}\hat{J}_z^{10}\}, \{\hat{J}_+^2 + \hat{J}_-^2\}]_+. \quad (1)$$

The only difference between this expression and Eq. (8) of Ref. (*1*) is that a number of higher order terms have been included here in order to fit the data. The derived

TABLE I

Rotational and Centrifugal Distortion Constants of H_2Se in the Ground State

		$H_2{}^{82}Se$	$H_2{}^{80}Se$	$H_2{}^{78}Se$	$H_2{}^{77}Se$	$H_2{}^{76}Se$	$H_2{}^{74}Se$
$(B+C)/2$	$\times 10^{-3}$	174.289127(18)	174.306090(20)	174.323954(19)	174.333215(20)	174.342757(19)	174.362523(25)
$A-(B+C)/2$	$\times 10^{-3}$	70.4902933(68)	70.6201935(55)	70.7566949(65)	70.8274563(72)	70.9003391(55)	71.0516495(74)
$(B-C)/2$	$\times 10^{-3}$	57.3564961(74)	57.3396905(60)	57.3220400(61)	57.3128918(81)	57.3034850(74)	57.2839445(91)
D_J		*15.83723(31)*	*15.83668(19)*	*15.83696(29)*	*15.83761(39)*	*15.83794(42)*	*15.83940(73)*
D_{JK}		−55.42555(22)	−55.435728(98)	−55.44472(15)	−55.44593(35)	−55.44934(24)	−55.45931(66)
D_K		78.992336(142)	79.048994(71)	79.10608(11)	79.13347(31)	79.163872(171)	79.22923(60)
d_1		7.271084(100)	7.270695(42)	7.270285(65)	7.27032(12)	7.270374(111)	7.26980(23)
d_K		−5.51076(21)	−5.495655(79)	−5.47983(13)	−5.47315(24)	−5.465301(172)	−5.44790(56)
H_J	$\times 10^3$	6.49726(152)	6.49174(61)	6.4807(11)	6.4819(24)	6.4821(22)	6.4880(35)
H_{JK}	$\times 10^3$	−37.31509(183)	−37.36206(35)	−37.33599(75)	−37.2922(19)	−37.29884(206)	−37.3141(44)
H_{KJ}	$\times 10^3$	38.51495(150)	38.52029(26)	38.36177(50)	38.343275(120)	38.35325(147)	38.3383(100)
H_K	$\times 10^3$	13.41005(157)	13.47893(24)	13.62504(50)	13.6314(16)	13.6537(15)	13.7359(91)
h_J	$\times 10^3$	3.23874(64)	3.23351(13)	3.22998(26)	3.23028(77)	3.23087(53)	3.2257(24)
h_{JK}	$\times 10^3$	−12.2133(23)	−12.19267(36)	−12.20517(88)	−12.2016(27)	−12.1954(16)	−12.1895(67)
h_K	$\times 10^3$	23.5598(48)	23.58411(84)	23.6788(15)	23.6551(60)	23.6657(38)	23.731(13)
c_{40}	$\times 10^6$	*−4.2026(48)*	*−4.1924(18)*	*−4.1258(31)*	*−4.1154(82)*	*−4.1174(69)*	*−4.1276(71)*
c_{31}	$\times 10^6$	17.310(35)	17.5530(42)	17.746(12)	17.569(50)	17.629(27)	17.629[c]
c_{22}	$\times 10^6$	−10.983(55)	−10.3415(86)	−10.185(16)	−10.742(60)	−10.649(35)	−10.649[c]
c_{13}	$\times 10^6$	23.716(51)	24.0543(57)	25.514(14)	24.957(66)	24.818(49)	24.807(28)
c_{04}	$\times 10^6$	−17.3002(43)	−17.28133(34)	−17.05733(91)	−17.1250(51)	−17.1665(30)	−17.257(29)
b_{30}	$\times 10^6$	−2.1056(33)	−2.08328(96)	−2.0684(17)	−2.0651(40)	−2.0671(31)	−2.0542(69)
b_{21}	$\times 10^6$	5.976(20)	5.9872(28)	6.1339(60)	6.137(25)	6.107(12)	6.158(69)
b_{12}	$\times 10^6$	0.1908[a]	0.1908(34)	0.4156(78)	0.4156[b]	0.4156[b]	0.4156[b]
b_{03}	$\times 10^6$	−24.876(37)	−24.9812(54)	−25.661(12)	−25.369(43)	−25.394(30)	−25.75(13)
c_{50}	$\times 10^9$	2.856(11)	2.8456(63)	2.7221(96)	2.687(15)	2.691(14)	2.691[c]
c_{41}	$\times 10^9$	−12.38(13)	−12.798(21)	−13.583(61)	−13.31(17)	−13.43(10)	−13.43[c]
c_{32}	$\times 10^9$						
c_{23}	$\times 10^9$	23.66(40)	20.201(35)	18.557(85)	21.93(38)	21.23(27)	21.23[c]
c_{14}	$\times 10^9$	−31.94(24)	−31.391(31)	−38.044(96)	−37.71(28)	−37.01(24)	−37.01[c]
c_{05}	$\times 10^9$	16.576(13)	16.51157(75)	15.7883(23)	15.886(13)	15.9215(67)	15.9215[c]
b_{40}	$\times 10^9$	1.4320(69)	1.4001(36)	1.3800(41)	1.3698(81)	1.3708(71)	1.3708[c]
b_{31}	$\times 10^9$	−4.338(79)	−4.2914(96)	−4.549(22)	−4.731(79)	−4.569(59)	−4.569[c]
b_{22}	$\times 10^9$	5.19(18)	4.059(24)	3.289(39)	4.31(23)	3.68(16)	3.68[c]
b_{13}	$\times 10^9$	−6.83(15)	−6.027(17)	−6.393(42)	−7.23(19)	−6.896(132)	−6.896[c]
b_{04}	$\times 10^9$	34.760(92)	34.702(12)	37.442(65)	36.85(10)	36.750(84)	36.750[c]
c_{60}	$\times 10^{12}$	−1.132[a]	−1.132(10)	−1.077(12)	−1.077[b]	−1.077[b]	−1.077[b]
c_{51}	$\times 10^{12}$	2.294[a]	2.294(55)	2.89(15)	2.89[b]	2.89[b]	2.89[b]
c_{42}	$\times 10^{12}$						
c_{33}	$\times 10^{12}$						
c_{24}	$\times 10^{12}$						
c_{15}	$\times 10^{12}$	16.575[a]	16.575(91)	29.05(32)	29.05[b]	29.05[b]	29.05[b]
c_{06}	$\times 10^{12}$	−14.2857[a]	−14.2857(15)	−13.6285(47)	−13.6285[b]	−13.6285[b]	−13.6285[b]
b_{50}	$\times 10^{12}$	−0.5455[a]	−0.5455(59)	−0.5464(53)	−0.5464[b]	−0.5464[b]	−0.5464[b]
b_{41}	$\times 10^{12}$						
b_{32}	$\times 10^{12}$						
b_{23}	$\times 10^{12}$						
b_{14}	$\times 10^{12}$						
b_{05}	$\times 10^{12}$	−24.261[a]	−24.261(14)	−28.213(97)	−28.213[b]	−28.213[b]	−28.213[b]
c_{07}	$\times 10^{15}$	7.2677[a]	7.2677(28)	7.2677[a]	7.2677[a]	7.2677[a]	7.2677[a]
Total Num. of Trans.		489	685	636	481	487	149
Num. of Fitted MW Trans.		59	83	72	57	59	36
Total Num. of IR Trans.		430	602	564	424	428	113
Num. of Fitted IR Trans.		406	577	537	400	406	105
Std.Dev. of MW Trans.		1.026	1.078	0.912	0.848	0.752	0.845
Std.Dev. of IR Trans.		0.517	0.737	0.610	0.530	0.609	0.627

All parameters are given in MHz. Value in parenthesis is one standard deviation in last digits of parameter. The blank entry means that the constant was fixed to zero.

[a] Value of parameter was fixed equal to the value of corresponding $H_2{}^{80}Se$ constant.

[b] Value of parameter was fixed equal to the value of corresponding $H_2{}^{78}Se$ constant.

[c] Value of parameter was fixed equal to the value of corresponding $H_2{}^{76}Se$ constant.

constants are presented in Table I. Due to the large amount of measured data, we will not publish all of them. Table II reproduces the fitted MW frequencies and FIR wavenumbers for $H_2{}^{80}Se$ only (the most abundant isotopic modification of H_2Se). However all data are available from the authors on a 5.25-inch, 1.2 MB, MS-DOS-format diskette. A copy of this diskette has been deposited with the editorial office of this journal.

DISCUSSION

Basically the fourfold clustering effect in the H_2Se molecule can be explained by means of a simple bending model, as was done for H_2O in Ref. (*11*) in a classical approach and in Ref. (*12*) in a quantum approach. A more general semiclassical treatment of clustering effects involves a rotational energy surface (RES) analysis (*1, 13, 14*). The structure of the RES changes as J increases, and this causes the fourfold clusters. Four "newborn" maxima appear on the RES at $J = J_{CR}$ instead of the two "old" maxima present for lower J so that for $J > J_{CR}$, the "old" a-axis is replaced by two new precession axes (Fig. 2). Since the b-axis is the C_{2v} axis of symmetry, the appearance of the new precession axes gives rise to four equivalent precession motions. The transition from the topologically conventional RES (the RES of an ordinary asymmetric top molecule with two maxima and two minima) to the RES with four maxima is caused by the C_{2v}-type local bifurcation according to the classification of Ref. (*14*). The analysis of the RES dynamics with increasing J has shown that the angle between the a-axis and the new precession axis tends to be constant (*1*).

The tunneling between equivalent states leads to level clusters. For any J value of an almost rigid asymmetric-top molecule (*13*), or for H_2Se with $J < J_{CR}$, twofold clusters (doublets) are formed, but for H_2Se with $J > J_{CR}$, we observe fourfold clusters of levels. For an almost rigid asymmetric-top molecule we know that if J is high the rotational wavefunctions are sharply localized around the axes with maximum and minimum moment of inertia (by standard notation these axes are the c- and a-axes, respectively). The localization of rotational states is reflected in the fact that the K_a (or K_c) quantum number becomes rather "good". In particular, the wavefunctions $|JK = J\rangle \pm |JK = -J\rangle$ become increasingly better approximations for the eigenfunctions of the highest (lowest) rotational doublet of the J-multiplet. This follows directly from the fact that in the classical limit the total angular momentum of the highest (lowest) state must have the largest probability of being found along the axis of precession. That is not true for H_2Se with $J > J_{CR}$. In this case, the rotational eigenfunctions are expressed as a linear combination $\sum a_K|JK\rangle$ of symmetric top basis functions (with the a-axis as a quantum axis). In Fig. 3a we present the a_K-expansion coefficients for the $23_{23\,0}$ state of $H_2{}^{80}Se$, plotted against K. The figure shows that in this state there is heavy mixing of basis functions and that the maximum contribution occurs for $K = 21$ and not, as one would perhaps expect, for $K = 23$. However it follows from the semi-classical analysis that the "cluster" wavefunctions with $J > J_{CR}$ must be localized around precession axes that are rotated relative to the original a-axis (*1, 14*), and this classical analogy provides us with four possible equivalent trajectories of the end point of the total angular momentum vector in the molecular-fixed coordinate system (Fig. 2). When the angular momentum lies along the precession axis, the trajectory is reduced to a point. The four trajectories can be compared to four quantum states for the fourfold cluster of highest energy,

TABLE II

Rotational Transitions in the Ground State of $H_2{}^{80}Se$

Obs. Freq.	Obs.-Calc.	Unc.	J Ka Kc lower	J Ka Kc upper	Obs. Freq.	Obs.-Calc.	Unc.	J Ka Kc lower	J Ka Kc upper
75706.329 a	0.013	0.5E-01	6 4 3	7 1 6	614973.030	-0.017	0.1E+00	5 3 3	5 4 2
118514.970 a	0.102	0.1E+00	23 22 1	23 23 0	615663.219	0.090	0.1E+00	14 13 1	14 14 0
118609.050 a	-0.081	0.2E+00	23 22 2	23 23 1	617320.055	-0.043	0.1E+00	10 9 2	10 10 1
125902.019 a	-0.005	0.1E+00	3 2 1	4 1 4	622313.853	-0.083	0.1E+00	13 12 1	13 13 0
127973.567 a	-0.013	0.2E-01	1 0 1	1 1 0	624973.383	0.040	0.1E+00	6 4 3	6 5 2
142172.116 a	0.025	0.2E-01	2 1 1	2 2 0	629639.398	-0.083	0.1E+00	14 13 2	14 14 1
165240.407 a	-0.013	0.2E-01	3 2 1	3 3 0	631533.596	-0.153	0.1E+00	12 10 2	12 11 1
169753.590 a	0.027	0.1E+00	22 21 1	22 22 0	635018.707	-0.089	0.1E+00	14 10 4	14 11 3
169955.083 a	-0.046	0.5E-01	22 21 2	22 22 1	635737.460	0.224	0.1E+00	13 9 4	13 10 3
198776.380 b	0.007	0.1E+00	4 3 1	4 4 0	636338.420	-0.181	0.1E+00	11 10 2	11 11 1
243754.690 b	-0.068	0.1E+00	5 4 1	5 5 0	640271.353	0.128	0.1E+00	7 5 3	7 6 2
299490.160 b	-0.065	0.1E+00	6 5 1	6 6 0	643956.435	-0.177	0.1E+00	13 12 2	13 13 1
305959.970	-0.117	0.1E+00	5 4 2	6 1 5	645781.022	-0.076	0.2E+00	12 11 2	12 12 1
302316.342	0.211	0.1E+00	20 19 2	20 20 1	35.227349	-0.000177	0.2E-03	3 1 3	4 0 4
307884.720 b	-0.021	0.1E+00	5 3 2	5 4 1	35.231568	-0.000074	0.2E-03	3 0 3	4 1 4
309399.660 b	-0.069	0.1E+00	6 4 2	6 5 1	42.518772	-0.000180	0.2E-03	11 5 6	11 6 5
316164.200 b	0.003	0.1E+00	4 2 2	4 3 1	43.017285	-0.000011	0.2E-03	4 1 4	5 0 5
318632.705 c	-0.013	0.1E+00	8 5 4	9 2 7	43.017285	-0.000373	0.2E+13	4 0 4	5 1 5
323130.689 c	0.051	0.1E+00	8 4 4	9 3 7	43.081071	-0.000132	0.2E-03	10 5 6	10 6 5
324255.520 b	-0.101	0.1E+00	7 5 2	7 6 1	43.162429	-0.000099	0.2E-03	3 2 2	4 1 3
329992.710 b	-0.064	0.1E+00	3 1 2	3 2 1	43.414224	-0.000206	0.2E-03	3 1 2	4 2 3
332715.474 c	-0.064	0.1E+00	11 5 6	12 4 9	43.731128	-0.000186	0.2E-03	8 2 6	8 3 5
332178.264 c	0.049	0.1E+00	11 6 6	12 3 9	43.739337	-0.000114	0.2E-03	8 3 6	8 4 5
336187.653	-0.153	0.5E+00	2 2 0	3 1 3	44.014163	-0.000102	0.2E-03	7 1 6	7 2 5
344953.150 b	-0.037	0.1E+00	2 0 2	2 1 1	44.016242	0.000024	0.2E-03	7 2 6	7 3 5
350168.400	-1.028	0.7E+00	5 3 2	6 2 5	44.255721	0.000085	0.2E-03	6 0 6	6 1 5
355087.300 b	-0.102	0.1E+00	8 6 2	8 7 1	44.888159	-0.000166	0.2E-03	2 2 0	3 3 1
361879.280 b	0.061	0.1E+00	0 0 0	1 1 1	49.427235	-0.000129	0.2E-03	3 3 1	4 2 2
362998.900 b	-0.098	0.1E+00	7 6 1	7 7 0	50.320745	-0.000088	0.2E-03	12 6 7	12 7 6
373816.770	0.172	0.1E+00	19 18 1	19 19 0	50.768080	-0.000079	0.2E-03	11 4 7	11 5 6
375107.100	-0.336	0.1E+01	19 18 2	19 19 1	50.799953	-0.000174	0.2E-03	5 1 5	6 0 6
383463.650 b	-0.019	0.1E+00	2 1 2	2 2 1	50.799953	-0.000209	0.2E-03	5 0 5	6 1 6
402553.930 b	0.008	0.1E+00	3 2 2	3 3 1	51.041463	-0.000122	0.2E-03	4 2 3	5 1 4
403259.550 b	-0.041	0.1E+00	9 7 2	9 8 1	51.070637	-0.000066	0.2E-03	4 1 3	5 2 4
427295.160 b	0.014	0.1E+00	4 3 2	4 4 1	51.165989	-0.000094	0.2E-03	2 2 1	3 3 0
429235.840 b	-0.035	0.1E+00	8 7 1	8 8 0	51.599899	0.000098	0.2E-03	9 2 7	9 3 6
443219.066	-0.063	0.1E+00	18 17 1	18 18 0	51.599899	-0.001274	0.2E+13	9 3 7	9 4 6
445382.771	-0.438	0.1E+00	18 17 2	18 18 1	51.951223	0.000110	0.2E+13	8 1 7	8 2 6
456827.960 b	0.035	0.1E+00	5 4 2	5 5 1	51.951223	-0.000176	0.2E-03	8 2 7	8 3 6
468076.442	0.129	0.1E+00	10 8 2	10 9 1	52.263095	-0.000059	0.2E-03	7 0 7	7 1 6
474150.381	-0.173	0.1E+00	10 7 3	10 8 2	52.263095	-0.000101	0.2E-03	7 1 7	7 2 6
479411.997	-0.089	0.1E+00	9 6 3	9 7 2	52.733042	-0.000087	0.2E-03	3 2 1	4 3 2
487728.666	-0.038	0.1E+00	11 8 3	11 9 2	58.445124	-0.000103	0.2E-03	2 1 2	3 2 1
489861.690 b	0.066	0.1E+00	6 5 2	6 6 1	58.576355	-0.000107	0.2E-03	6 1 6	7 0 7
492152.550 b	0.037	0.1E+00	9 8 1	9 9 0	58.576355	-0.000110	0.2E-03	6 0 6	7 1 7
498190.965	-0.058	0.1E+00	8 5 3	8 6 2	58.717549	-0.000070	0.2E-03	4 3 2	5 2 3
505083.138	0.158	0.1E+00	17 16 1	17 17 0	58.821138	-0.000025	0.2E-03	5 2 4	6 1 5
508610.322	-0.151	0.1E+00	17 16 2	17 17 1	58.824297	-0.000132	0.2E-03	5 1 4	6 2 5
523529.039	0.108	0.1E+00	12 9 3	12 10 2	58.950863	0.000161	0.2E-03	11 3 8	11 4 7
524110.606	0.060	0.1E+00	7 4 3	7 5 2	58.950863	-0.000859	0.2E+13	11 4 8	11 5 7
524657.702	0.125	0.1E+00	7 6 2	7 7 1	59.424659	-0.000152	0.2E-03	10 3 8	10 4 7
546105.709	0.130	0.1E+00	11 9 2	11 10 1	59.424659	0.000087	0.2E+13	10 2 8	10 3 7
546126.707	-0.058	0.1E+00	10 9 1	10 10 0	59.480185	-0.000069	0.2E-03	4 2 2	5 3 3
550936.685	0.062	0.1E+00	6 3 3	6 4 2	59.859313	-0.000042	0.2E-03	9 1 8	9 2 7
555879.552	0.485	0.2E+00	16 15 1	16 16 0	59.859313	-0.000086	0.2E-03	9 2 8	9 3 7
559092.556	0.145	0.1E+00	8 7 2	8 8 1	60.255029	-0.000014	0.2E-03	8 0 8	8 1 7
561525.259	0.010	0.1E+00	16 15 2	16 16 1	60.255029	-0.000020	0.2E-03	8 1 8	8 2 7
573860.601	0.037	0.1E+00	5 2 3	5 3 2	61.136992	-0.000083	0.2E-03	2 0 2	3 3 1
581098.890 b	0.117	0.1E+00	1 1 1	2 0 2	61.474261	-0.000073	0.2E-03	3 3 0	4 4 1
582078.184	0.007	0.1E+00	13 10 3	13 11 2	63.606426	-0.000089	0.2E-03	4 4 1	5 3 2
587082.693	-0.008	0.1E+00	11 10 1	11 11 0	66.034831	-0.000638	0.2E-03	13 5 9	13 6 8
590368.962	-0.016	0.1E+00	4 1 3	4 2 2	66.345314	-0.000071	0.2E-03	7 0 7	8 1 8
590794.173	0.096	0.1E+00	9 8 2	9 9 1	66.345314	-0.000070	0.2E-03	7 1 7	8 0 8
593231.881	0.206	0.1E+00	15 14 1	15 15 0	66.583688	0.000046	0.2E-03	6 2 5	7 1 6
595800.970 b	0.077	0.1E+00	1 0 1	2 1 2	66.583688	-0.000337	0.2E+13	6 1 5	7 2 6
600323.160	-0.093	0.1E+00	3 0 3	3 1 2	66.762330	-0.000080	0.2E-03	5 3 3	6 2 4
602159.265	0.079	0.1E+00	15 14 2	15 15 1	66.879681	-0.000057	0.2E-03	5 2 3	6 3 4
606976.357	-0.040	0.1E+00	3 1 3	3 2 2	67.208889	-0.000048	0.2E-03	11 2 9	11 3 8
609360.340	0.016	0.1E+00	4 2 3	4 3 2	67.208889	-0.000092	0.2E-03	11 3 9	11 4 8
612767.520	0.139	0.1E+00	12 11 1	12 12 0	67.739399	-0.000066	0.2E-03	10 1 9	10 2 8

All values are given in MHZ for MW data, in cm^{-1} for FIR data. MW frequencies were taken from Ref.(1) if not marked.

a Ref.(2).

b Ref.(7).

c frequency measured in Ref.(1) but not included in final fit there. In the case of unresolved doublet components the smallest component was not included in the fit (an uncertainty of 0.2E+13 cm^{-1} was given) if a predicted splitting exceeded 0.0001 cm^{-1}.

TABLE II—*Continued*

Obs. Freq.	Obs.-Calc.	Unc.	J	Ka	Kc	J	Ka	Kc	Obs. Freq.	Obs.-Calc.	Unc.	J	Ka	Kc	J	Ka	Kc
			lower			upper						lower			upper		
67.739399	-0.000074	0.2E-03	10	2	9	10	3	8	97.696276	*0.000014*	*0.2E-03*	9	3	7	*10*	2	8
68.230951	0.000032	0.2E-03	9	0	9	9	1	8	97.699546	-0.000092	0.2E-03	7	5	3	8	4	4
68.230951	0.000031	0.2E-03	9	1	9	9	2	8	97.849984	-0.000074	0.2E-03	8	4	5	9	3	6
69.447369	-0.000075	0.2E-03	4	3	1	5	4	2	97.859881	-0.000023	0.2E-03	8	3	5	9	4	6
73.963272	-0.000014	0.2E-03	5	4	2	6	3	3	97.938336	-0.000117	0.2E-03	15	2	13	15	3	12
74.106184	0.000303	0.2E-03	8	0	8	9	1	9	97.938336	-0.000117	0.2E-03	15	3	13	15	4	12
74.106184	0.000303	0.2E-03	8	1	8	9	0	9	98.185570	-0.000050	0.2E-03	4	2	3	5	3	2
74.278894	-0.000004	0.2E-03	13	3	10	13	4	9	98.575315	-0.000062	0.2E-03	7	4	3	8	5	4
74.278894	-0.000048	0.2E-03	13	4	10	13	5	9	98.965536	-0.000124	0.2E-03	14	1	13	14	2	12
74.337204	-0.000028	0.2E-03	7	2	6	8	1	7	*98.965536*	*-0.000124*	*0.2E-03*	*14*	2	13	14	3	12
74.337204	-0.000076	0.2E-03	7	1	6	8	2	7	99.686064	-0.000072	0.2E-03	4	1	3	5	4	2
74.540439	-0.000053	0.2E-03	6	3	4	7	2	5	99.961624	*0.000179*	*0.2E-03*	*13*	*0*	13	*13*	*1*	12
74.556798	-0.000058	0.2E-03	6	2	4	7	3	5	99.961624	0.000179	0.2E-03	13	1	13	13	2	12
74.953153	-0.000043	0.2E-03	12	3	10	12	4	9	102.034081	-0.000061	0.2E-03	7	7	1	8	6	2
74.953153	-0.000034	0.2E-03	12	2	10	12	3	9	102.660955	-0.000062	0.2E-03	5	4	2	6	5	1
75.590887	-0.000088	0.2E-03	11	2	10	11	3	9	102.916946	-0.000025	0.2E-03	7	6	2	8	5	3
75.590887	-0.000087	0.2E-03	11	1	10	11	2	9	103.286097	-0.000063	0.2E-03	6	5	1	7	6	2
75.738655	-0.000091	0.2E-03	5	3	2	6	4	3	*105.043255*	*-0.000042*	*0.2E-03*	*12*	*0*	*12*	*13*	*1*	13
76.190206	0.000023	0.2E-03	10	0	10	10	1	*9*	*105.043255*	*-0.000042*	*0.2E-03*	*12*	*1*	12	13	*0*	13
76.190206	0.000023	0.2E-03	10	1	10	10	2	9	105.250654	0.000007	0.2E-03	11	1	10	12	2	11
77.102356	-0.000058	0.2E-03	5	5	1	6	4	2	105.250654	0.000007	0.2E-03	11	2	10	12	1	11
77.993562	0.000027	0.2E-03	3	1	2	4	4	1	105.390973	-0.000046	0.2E-03	10	2	8	11	3	9
78.055082	-0.000036	0.2E-03	4	4	0	5	5	1	105.390973	-0.000037	0.2E-03	10	3	8	11	2	9
81.856848	-0.000085	0.2E-03	9	0	9	10	1	10	105.519704	0.000043	0.2E-03	9	4	6	10	3	7
81.856848	-0.000085	0.2E-03	9	1	9	10	0	10	105.521356	0.000032	0.2E-03	9	3	6	10	4	7
82.007209	-0.000019	0.2E-03	4	4	1	5	5	0	105.627507	-0.000026	0.2E-03	8	5	4	9	4	5
82.081712	-0.000039	0.2E-03	8	2	7	9	1	8	105.806076	-0.000067	0.2E-03	8	4	4	9	5	5
82.081712	-0.000046	0.2E-03	8	1	7	9	2	8	*106.693580*	*-0.000383*	*0.2E-03*	*15*	*1*	*14*	15	2	13
82.272060	-0.000066	0.2E-03	7	3	5	8	2	6	106.693580	-0.000383	0.2E-03	15	2	14	15	3	13
82.274371	-0.000043	0.2E-03	7	2	5	8	3	6	107.251062	-0.000047	0.2E-03	4	1	4	5	2	3
82.340252	-0.000091	0.2E-03	6	4	3	7	3	4	107.354312	-0.000086	0.2E-03	4	0	4	5	3	3
82.656704	-0.000095	0.2E-03	13	3	11	13	4	10	107.847484	0.000218	0.2E-03	14	0	14	14	1	13
82.656704	*-0.000093*	*0.2E-03*	*13*	*2*	*11*	13	*3*	*10*	*107.847484*	*0.000218*	*0.2E-03*	*14*	*1*	14	14	2	13
82.692868	-0.000089	0.2E-03	6	3	3	7	4	4	109.032872	-0.000103	0.2E-03	7	5	2	8	6	3
83.101609	-0.000062	0.2E-03	3	1	3	4	2	2	110.796890	-0.000044	0.2E-03	6	6	0	7	7	1
83.413046	-0.000079	0.2E-03	12	2	11	12	3	10	112.729748	-0.000039	0.2E-03	8	6	3	9	5	4
83.413046	-0.000079	0.2E-03	*12*	*1*	*11*	12	2	10	*112.819674*	*-0.000085*	*0.2E-03*	*6*	*6*	*1*	7	7	*0*
83.765076	-0.000055	0.2E-03	3	0	3	4	3	2	112.853928	0.000082	0.2E-03	5	3	3	6	4	2
84.132254	0.000088	0.2E-03	11	0	11	11	1	10	112.925593	-0.000045	0.2E-03	5	3	2	6	6	1
84.132254	0.000088	0.2E-03	11	1	11	11	2	10	112.948612	0.000032	0.2E-03	12	1	11	13	2	12
86.108535	-0.000093	0.2E-03	7	7	0	8	6	3	112.948612	0.000032	0.2E-03	12	2	11	13	1	12
86.315635	-0.000049	0.2E-03	5	4	1	6	5	2	113.072779	-0.000017	0.2E-03	11	3	9	12	2	10
88.129288	-0.000189	0.2E-03	4	3	2	5	4	1	113.072779	-0.000019	0.2E-03	11	2	9	12	3	10
88.752914	-0.000077	0.2E-03	6	5	2	7	4	3	113.175183	-0.000244	0.2E+13	10	3	7	11	4	8
89.401249	0.000045	0.2E-03	15	4	12	15	5	11	113.175183	0.000047	0.2E-03	10	4	7	11	3	8
89.401249	0.000047	0.2E-03	15	3	12	15	4	*11*	*113.300318*	*0.000063*	*0.2E-03*	*9*	5	5	*10*	4	6
89.597411	-0.000115	0.2E-03	10	0	10	11	1	11	113.334482	0.000130	0.2E-03	9	4	5	10	5	6
89.597411	*-0.000115*	0.2E-03	*10*	*1*	*10*	11	0	11	113.422796	-0.000008	0.2E-03	9	9	0	10	8	3
89.816165	-0.000032	0.2E-03	9	1	8	10	2	9	113.629510	-0.000026	0.2E-03	8	8	1	9	7	2
89.816165	-0.000031	0.2E-03	9	2	8	10	1	9	114.388214	-0.000550	0.2E-03	16	1	15	16	2	14
89.895373	-0.000039	0.2E-03	6	6	1	7	5	2	114.388214	-0.000550	0.2E-03	16	2	15	16	3	14
89.989760	0.000053	0.2E-03	8	3	6	9	2	7	114.621099	-0.000042	0.2E-03	8	5	3	9	6	4
89.989760	-0.000285	0.2E+13	8	2	6	9	3	7	115.713154	0.000293	0.2E-03	15	0	15	15	1	14
90.153128	-0.000043	0.2E-03	7	4	4	8	3	5	115.713154	0.000293	0.2E-03	15	1	15	15	2	14
90.213033	-0.000044	0.2E-03	7	3	4	8	4	5	115.727485	*-0.000056*	*0.2E-03*	5	2	3	*6*	5	2
90.318796	-0.000111	0.2E-03	14	3	12	14	4	11	116.287364	-0.000021	0.2E-03	8	7	2	9	6	3
90.318796	-0.000111	0.2E-03	14	2	12	14	3	11	117.051420	-0.000020	0.2E-03	6	5	2	7	6	1
91.204914	-0.000106	0.2E-03	13	2	12	13	3	11	120.278651	-0.000064	0.2E-03	7	6	1	8	7	2
91.204914	-0.000106	0.2E-03	13	1	12	13	2	11	120.435217	0.000053	0.2E-03	14	0	14	15	1	15
92.056303	0.000140	0.2E-03	12	0	12	12	1	11	120.435217	0.000053	0.2E-03	14	1	14	15	0	15
92.056303	0.000140	0.2E-03	12	1	12	12	2	11	120.632337	0.000049	0.2E-03	13	2	12	14	1	13
92.249424	-0.000051	0.2E-03	6	4	2	7	5	3	120.632337	0.000049	0.2E-03	13	1	12	14	2	13
94.524871	-0.000054	0.2E-03	5	5	0	6	6	1	120.740726	0.000251	0.2E-03	12	2	10	13	3	11
95.231627	-0.000059	0.2E-03	4	2	2	5	5	1	*120.740726*	*0.000251*	*0.2E-03*	*12*	*3*	*10*	13	2	*11*
97.326601	-0.000049	0.2E-03	11	0	11	12	1	12	120.913871	0.000350	0.2E-03	10	5	6	11	4	7
97.326601	-0.000049	0.2E-03	11	1	11	12	0	12	120.920064	0.000002	0.2E-03	10	4	6	11	5	7
97.412768	-0.000028	0.2E-03	5	5	1	6	6	0	121.373245	-0.000011	0.2E-03	9	5	4	10	6	5
97.539481	-0.000028	0.2E-03	10	1	9	11	2	10	122.578668	*-0.000051*	*0.2E-03*	5	2	4	6	3	3
97.539481	-0.000028	0.2E-03	10	2	9	11	1	10	122.882724	-0.000057	0.2E-03	5	1	4	6	4	3
97.696276	-0.000038	0.2E-03	9	2	7	10	3	8	123.557753	0.000302	0.2E-03	16	0	16	16	1	15

$$R_c^{\varphi} \,|\, JK = JM\rangle = |1\rangle \tag{2}$$

$$R_b^{\pi} \,|\, 1\rangle = |2\rangle \tag{3}$$

$$R_c^{\pi} \,|\, 1\rangle = |3\rangle \tag{4}$$

TABLE II—*Continued*

Obs. Freq.	Obs.-Calc.	Unc.	J	Ka	Kc	J	Ka	Kc	Obs. Freq.	Obs.-Calc.	Unc.	J	Ka	Kc	J	Ka	Kc
			lower			upper						lower			upper		
123.557753	0.000302	0.2E-03	16	1	16	16	2	15	151.204719	-0.000003	0.2E-03	17	1	16	18	2	17
124.848130	-0.000048	0.2E-03	9	9	1	10	8	2	151.223233	-0.000324	0.2E-03	15	4	12	16	3	13
126.066947	-0.000034	0.2E-03	8	6	2	9	7	3	151.223233	-0.000324	0.2E-03	15	3	12	16	4	13
126.819664	-0.000023	0.2E-03	7	7	0	8	8	1	151.234436	0.000074	0.2E-03	12	7	6	13	6	7
127.082163	-0.000141	0.2E-03	6	4	3	7	5	2	151.247779	-0.000244	0.2E-03	16	3	14	17	2	15
127.279008	-0.000056	0.2E-03	9	7	3	10	6	4	151.247779	-0.000244	0.2E-03	16	2	14	17	3	15
128.108456	0.000060	0.2E-03	15	1	15	16	0	16	152.207896	-0.000010	0.2E-03	7	4	4	8	5	3
128.108456	0.000060	0.2E-03	15	0	15	16	1	16	152.755775	0.000062	0.2E-03	11	7	4	12	8	5
128.196299	-0.000051	0.2E-03	7	7	1	8	8	0	153.774823	-0.000112	0.2E-03	7	3	4	8	6	3
128.300810	0.000051	0.2E-03	14	2	13	15	1	14	153.886460	0.000009	0.2E-03	9	8	1	10	9	2
128.300810	0.000051	0.2E-03	14	1	13	15	2	14	154.148130	0.000011	0.2E-03	11	9	3	12	8	4
128.392877	-0.000051	0.2E-03	13	3	11	14	2	12	154.340594	-0.000001	0.2E-03	8	6	3	9	7	2
128.392877	-0.000051	0.2E-03	13	2	11	14	3	12	154.853835	-0.000045	0.2E-03	6	1	6	7	2	5
128.444040	-0.000047	0.2E-03	12	3	9	13	4	10	154.855977	0.000097	0.2E-03	6	0	6	7	3	5
128.444040	-0.000036	0.2E-03	12	4	9	13	3	10	158.061536	-0.000057	0.2E-03	9	9	0	10	10	1
128.506790	-0.000311	0.2E-03	11	4	7	12	5	8	158.599084	0.000054	0.2E-03	12	8	5	13	7	6
128.506790	0.000970	0.2E+13	11	5	7	12	4	8	158.627022	-0.000026	0.2E-03	19	1	19	20	0	20
128.600244	-0.000233	0.2E-03	10	6	5	11	5	6	158.627022	-0.000026	0.2E-03	19	0	19	20	1	20
128.701238	-0.000011	0.2E-03	10	5	5	11	6	6	158.657005	-0.000107	0.2E+13	14	5	9	15	6	10
128.738936	-0.000051	0.2E-03	9	8	2	10	7	3	158.657005	0.000137	0.2E-03	14	6	9	15	5	10
130.935405	-0.000024	0.2E-03	9	6	3	10	7	4	158.678364	0.000013	0.2E-03	9	9	1	10	10	0
131.099158	0.000007	0.2E-03	5	1	5	6	2	4	158.691847	0.000040	0.2E-03	13	6	7	14	7	8
131.113529	-0.000021	0.2E-03	5	0	5	6	3	4	158.778525	-0.000136	0.2E-03	16	4	13	17	3	14
131.983842	-0.000049	0.2E-03	6	3	3	7	6	2	158.778525	-0.000136	0.2E-03	16	3	13	17	4	14
135.765275	0.000095	0.2E-03	16	1	16	17	0	17	158.828512	-0.000166	0.2E-03	17	3	15	18	2	16
135.765275	0.000095	0.2E-03	16	0	16	17	1	17	158.828512	-0.000166	0.2E-03	17	2	15	18	3	16
135.937905	-0.000010	0.2E-03	10	7	4	11	6	5	159.221522	0.000052	0.2E-03	12	7	5	13	8	6
135.953060	0.000073	0.2E-03	15	2	14	16	1	15	160.168357	0.000065	0.2E-03	9	8	2	10	9	1
135.953060	0.000073	0.2E-03	15	1	14	16	2	15	160.604944	0.000022	0.2E-03	10	8	2	11	9	3
136.054996	-0.000042	0.2E-03	13	3	10	14	4	11	160.623526	0.000114	0.2E-03	12	11	2	13	10	3
136.054996	-0.000040	0.2E-03	13	4	10	14	3	11	161.483691	-0.000002	0.2E-03	7	3	5	8	4	4
136.082365	-0.000124	0.2E+13	12	4	8	13	5	9	161.635675	-0.000003	0.2E-03	7	2	5	8	5	4
136.082365	0.000137	0.2E-03	12	5	8	13	4	9	164.640295	0.000121	0.2E-03	11	8	3	12	9	4
136.157316	0.000008	0.2E-03	11	6	6	12	5	7	165.647743	0.000006	0.2E-03	8	5	3	9	8	2
136.179120	0.000026	0.2E-03	11	5	6	12	6	7	166.069446	0.000166	0.2E-03	12	10	3	13	9	4
136.986013	0.000022	0.2E-03	10	6	4	11	7	5	166.089001	0.000039	0.2E-03	14	7	8	15	6	9
137.185355	-0.000077	0.2E-03	8	7	1	9	8	2	166.092846	0.000144	0.2E-03	14	6	8	15	7	9
137.600771	-0.000023	0.2E-03	6	3	4	7	4	3	166.117835	-0.000030	0.2E-03	15	5	10	16	6	11
138.340890	-0.000020	0.2E-03	6	2	4	7	5	3	166.117835	0.000028	0.2E-03	15	6	10	16	5	11
140.227612	-0.000033	0.2E-03	10	9	2	11	8	3	166.121198	0.000091	0.2E-03	13	8	6	14	7	7
140.891983	-0.000001	0.2E-03	7	5	3	8	6	2	166.312549	-0.000137	0.2E-03	17	4	14	18	3	15
141.155851	-0.000026	0.2E-03	10	8	3	11	7	4	166.312549	-0.000137	0.2E-03	17	3	14	18	4	15
142.574408	-0.000025	0.2E-03	8	8	0	9	9	1	166.379549	0.000011	0.2E-03	19	2	18	20	1	19
143.290528	-0.000009	0.2E-03	9	7	2	10	8	3	166.379549	0.000011	0.2E-03	19	1	18	20	2	19
143.404625	0.000089	0.2E-03	17	1	17	18	0	18	166.388420	-0.000229	0.2E-03	18	3	16	19	2	17
143.404625	0.000089	0.2E-03	17	0	17	18	1	18	166.388420	-0.000229	0.2E-03	18	2	16	19	3	17
143.497261	-0.000008	0.2E-03	8	8	1	9	9	0	167.517860	0.000021	0.2E-03	9	7	3	10	8	2
143.588097	0.000124	0.2E-03	16	2	15	17	1	16	168.736745	0.000103	0.2E-03	8	6	2	9	9	1
143.588097	0.000124	0.2E-03	16	1	15	17	2	16	168.823398	0.000154	0.2E-03	12	8	4	13	9	5
143.642105	-0.000011	0.2E-03	13	4	9	14	5	10	169.259367	0.000041	0.2E-03	8	4	4	9	7	3
143.642105	0.000044	0.2E-03	13	5	9	14	4	10	170.019774	0.000116	0.2E-03	7	2	6	8	3	5
143.676946	0.000219	0.2E-03	12	6	7	13	5	8	170.028195	0.000065	0.2E-03	7	1	6	8	4	5
143.681500	0.000038	0.2E-03	12	5	7	13	6	8	170.279957	0.000193	0.2E-03	10	9	1	11	10	2
143.717740	0.000093	0.2E-03	11	7	5	12	6	6	173.160358	0.000241	0.2E-03	13	9	5	14	8	6
143.981003	0.000028	0.2E-03	11	6	5	12	7	6	173.288826	-0.000081	0.2E-03	10	10	0	11	11	1
145.730159	0.000016	0.2E-03	8	7	2	9	8	1	173.480805	-0.000076	0.2E-03	15	6	9	16	7	10
146.398687	-0.000008	0.2E-03	6	2	5	7	3	4	173.480805	0.000855	0.2E+13	15	7	9	16	6	10
146.450488	-0.000025	0.2E-03	6	1	5	7	4	4	173.536867	0.000133	0.2E-03	14	7	7	15	8	8
147.600307	0.000071	0.2E-03	10	7	3	11	8	4	173.557156	-0.000003	0.2E-03	16	5	11	17	6	12
148.577167	0.000002	0.2E-03	7	4	3	8	7	2	173.557156	0.000012	0.2E-03	16	6	11	17	5	12
149.744035	0.000001	0.2E-03	7	5	2	8	8	1	173.686060	-0.000020	0.2E-03	17	5	13	18	4	14
150.006691	0.000041	0.2E-03	6	4	3	7	7	0	173.686060	-0.000021	0.2E-03	17	4	13	18	5	14
150.581687	-0.000144	0.2E-03	11	8	4	12	7	5	173.704027	-0.000007	0.2E-03	10	10	1	11	11	0
151.025562	0.000076	0.2E-03	18	1	18	19	0	19	173.767976	0.000011	0.2E-03	21	1	21	22	0	22
151.025562	0.000076	0.2E-03	18	0	18	19	1	19	173.767976	0.000011	0.2E-03	21	0	21	22	1	22
151.176942	-0.000174	0.2E-03	13	5	8	14	6	9	173.824443	0.000072	0.2E-03	18	4	15	19	3	16
151.176942	0.000887	0.2E+13	13	6	8	14	5	9	173.824443	0.000072	0.2E-03	18	3	15	19	4	16
151.183845	-0.000001	0.2E-03	14	4	10	15	5	11	173.926584	-0.000225	0.2E-03	19	3	17	20	2	18
151.183845	0.000011	0.2E-03	14	5	10	15	4	11	173.926584	-0.000225	0.2E-03	19	2	17	20	3	18
151.204719	-0.000003	0.2E-03	17	2	16	18	1	17	173.935565	-0.000034	0.2E-03	20	2	19	21	1	2

$$R_a^{\pi}|1\rangle = |4\rangle, \tag{5}$$

where R_q^{θ} denotes a rotation through the angle θ around the q-axis ($q = a$, b, or c). Since we consider only the ground vibrational state, the D_2 rotational group can be used for classification of rotational states. The symmetrized wavefunctions

TABLE II—*Continued*

Obs. Freq.	Obs.-Calc.	Unc.	J	Ka	Kc	J	Ka	Kc
			lower			upper		
173.935565	-0.000034	0.2E-03	20	1	19	21	2	20
174.511177	0.000137	0.2E-03	13	8	5	14	9	6
174.712693	0.000048	0.2E-03	10	9	2	11	10	1
176.675922	0.000046	0.2E-03	8	3	5	9	6	4
177.872278	0.000082	0.2E-03	11	9	2	12	10	3
178.551815	-0.000018	0.2E-03	7	0	7	8	3	6
178.551815	0.000275	0.2E+13	7	1	7	8	2	6
179.765609	0.000027	0.2E-03	9	6	4	10	7	3
176.291501	-0.000144	0.2E-03	8	4	5	9	5	4
176.675850	-0.000026	0.2E-03	8	3	5	9	6	4
177.872223	0.000027	0.2E-03	11	9	2	12	10	3
178.015084	0.000101	0.2E-03	13	10	4	14	9	5
178.551707	0.000167	0.2E+13	7	1	7	8	2	6
178.551707	-0.000126	0.2E-03	7	0	7	8	3	6
179.765574	-0.000008	0.2E-03	9	6	4	10	7	3
180.543697	-0.000033	0.2E-03	10	8	3	11	9	2
180.779969	0.000074	0.2E-03	14	9	6	15	8	7
180.811988	0.000007	0.2E-03	15	8	8	16	7	9
180.823699	-0.000055	0.2E-03	15	7	8	16	8	9
180.849146	-0.000357	0.2E+13	16	6	10	17	7	11
180.849146	-0.000118	0.2E-03	16	7	10	17	6	11
180.973124	-0.000055	0.2E-03	17	5	12	18	6	13
180.973124	-0.000051	0.2E-03	17	6	12	18	5	13
181.141234	0.000219	0.2E-03	18	4	14	19	5	15
181.141234	0.000219	0.2E-03	18	5	14	19	4	15
181.185025	0.000015	0.2E-03	14	8	6	15	9	7
181.305176	0.000009	0.2E-03	22	0	22	23	1	23
181.305176	0.000009	0.2E-03	22	1	22	23	0	23
181.312813	0.000414	0.2E-03	19	3	16	20	4	17
181.312813	0.000414	0.2E-03	19	4	16	20	3	17
181.441986	-0.000002	0.2E-03	20	2	18	21	3	19
181.441986	-0.000002	0.2E-03	20	3	18	21	2	19
181.469346	-0.000031	0.2E-03	21	2	20	22	1	21
181.469346	-0.000031	0.2E-03	21	1	20	22	2	21
182.006713	0.000098	0.2E-03	12	9	3	13	10	4
183.329191	-0.000018	0.2E-03	9	6	3	10	9	2
184.208299	-0.000029	0.2E-03	8	6	3	9	9	0
184.901316	-0.000029	0.2E-03	9	5	4	10	8	3
184.988757	-0.000040	0.2E-03	8	3	6	9	4	5
185.017649	-0.000061	0.2E-03	8	2	6	9	5	5
185.322709	0.000022	0.2E-03	13	9	4	14	10	5
186.307836	-0.000018	0.2E-03	11	10	1	12	11	2
187.270158	0.000216	0.2E-03	14	10	5	15	9	6
187.929298	-0.000027	0.2E-03	9	7	2	10	10	1
188.103631	-0.000265	0.2E-03	16	8	9	17	7	10
188.106931	-0.000276	0.2E-03	15	9	7	16	8	8
188.224164	-0.000046	0.2E-03	15	8	7	16	9	8
188.265800	-0.000022	0.2E-03	11	11	0	12	12	1
188.549516	-0.000029	0.2E-03	11	11	1	12	12	0
189.335774	-0.000022	0.2E-03	11	10	2	12	11	1
190.329023	0.000187	0.2E-03	14	11	4	15	10	5
190.732225	-0.000022	0.2E-03	9	5	5	10	6	4
191.597079	0.000010	0.2E-03	9	4	5	10	7	4
192.621387	-0.000039	0.2E-03	10	7	4	11	8	3
193.540949	0.000041	0.2E-03	8	2	7	9	3	6
193.540949	-0.001381	0.2E+13	8	1	7	9	4	6
193.558261	-0.000024	0.2E-03	11	9	3	12	10	2
194.923199	0.000031	0.2E-03	12	10	2	13	11	3
196.053018	-0.000111	0.2E-03	15	9	6	16	10	7
199.579751	0.000105	0.2E-03	13	10	3	14	11	4
199.730547	-0.000022	0.2E-03	9	4	6	10	5	5
199.814822	-0.000021	0.2E-03	9	3	6	10	6	5
200.843721	0.000024	0.2E-03	10	6	4	11	9	3
201.708947	-0.000122	0.2E-03	10	7	3	11	10	2
201.962192	-0.000009	0.2E-03	12	11	1	13	12	2
202.196179	0.000024	0.2E-03	8	1	8	9	2	7
202.196179	-0.000021	0.2E-03	8	0	8	9	3	7
203.002545	-0.000016	0.2E-03	12	12	0	13	13	1
203.200764	-0.000022	0.2E-03	12	12	1	13	13	0
203.983551	-0.000015	0.2E-03	12	11	2	13	12	1
204.683934	-0.000031	0.2E-03	10	6	5	11	7	4
204.915852	-0.000034	0.2E-03	11	8	4	12	9	3
206.451251	0.000030	0.2E-03	10	5	5	11	8	4
206.691231	0.000002	0.2E-03	12	10	3	13	11	2
208.327899	-0.000021	0.2E-03	9	3	7	10	4	6
208.333456	0.000014	0.2E-03	9	2	7	10	5	6
211.586344	0.000045	0.2E-03	13	11	2	14	12	3
214.200643	0.000011	0.2E-03	10	5	6	11	6	5
214.417997	0.000014	0.2E-03	10	4	6	11	7	5
216.776048	-0.000044	0.2E-03	12	9	4	13	10	3
216.980376	-0.000105	0.2E-03	9	1	8	10	4	7
216.980376	0.000142	0.2E+13	9	2	8	10	3	7
217.176324	-0.000043	0.2E-03	14	11	3	15	12	4
217.260096	0.000046	0.2E-03	11	7	4	12	10	3
217.267132	-0.000014	0.2E-03	13	12	1	14	13	2
217.511525	0.000025	0.2E-03	13	13	0	14	14	1
217.653803	-0.000019	0.2E-03	13	13	1	14	14	0
218.005780	-0.000045	0.2E-03	11	7	5	12	8	4
218.342982	0.000160	0.2E-03	10	8	3	11	11	0
218.597623	0.000032	0.2E-03	13	12	2	14	13	1
220.018593	-0.000035	0.2E-03	13	11	3	14	12	2
220.792854	0.000000	0.2E-03	11	8	3	12	11	2
221.323736	0.000052	0.2E-03	11	6	5	12	9	4
222.894020	0.000023	0.2E-03	10	4	7	11	5	6
222.912173	0.000016	0.2E-03	10	3	7	11	6	6
225.786636	0.000055	0.2E-03	9	1	9	10	2	8
225.786636	0.000047	0.2E-03	9	0	9	10	3	8
226.065078	0.000164	0.2E-03	11	9	2	12	12	1
227.106470	0.000045	0.2E-03	10	7	4	11	10	1
227.730803	0.000102	0.2E-03	14	12	2	15	13	3
228.331858	0.000055	0.2E-03	11	6	6	12	7	5
228.839202	0.000002	0.2E-03	11	5	6	12	8	5
230.573577	-0.000040	0.2E-03	12	8	5	13	9	4
231.550933	-0.000788	0.2E+13	10	2	8	11	5	7
231.550933	0.000284	0.2E-03	10	3	8	11	4	7
231.809544	0.000137	0.2E-03	14	14	0	15	15	1
231.914844	0.000013	0.2E-03	14	14	1	15	15	0
232.259878	0.000028	0.2E-03	14	13	1	15	14	2
233.129240	-0.000024	0.2E-03	14	13	2	15	14	1
233.535816	-0.000026	0.2E-03	14	12	3	15	13	2
234.333426	0.000092	0.2E-03	12	8	4	13	11	3
234.566858	0.000141	0.2E-03	15	12	3	16	13	4
236.340772	0.000103	0.2E-03	12	7	5	13	10	4
237.215542	-0.000026	0.2E-03	11	5	7	12	6	6
237.268149	0.000063	0.2E-03	11	4	7	12	7	6
239.957651	-0.000095	0.2E-03	14	11	4	15	12	3
240.339430	-0.000035	0.2E-03	10	1	9	11	4	8
240.339430	0.000011	0.2E-03	10	2	9	11	3	8
242.023410	0.000078	0.2E-03	12	7	6	13	8	5
242.332631	-0.000034	0.2E-03	13	9	5	14	10	4
243.111438	0.000015	0.2E-03	12	6	6	13	9	5
243.293712	0.000102	0.2E-03	15	13	2	16	14	3
245.894063	0.000025	0.2E-03	11	4	8	12	5	7
245.898034	0.000079	0.2E-03	11	3	8	12	6	7
245.920007	0.000007	0.2E-03	15	15	0	16	16	1
246.977600	-0.000013	0.2E-03	15	14	1	16	15	2
249.320754	0.000089	0.2E-03	10	1	10	11	2	9
249.320754	0.000087	0.2E-03	10	0	10	11	3	9
242.023303	-0.000029	0.2E-03	12	7	6	13	8	5
242.332641	-0.000024	0.2E-03	13	9	5	14	10	4
243.111380	-0.000043	0.2E-03	12	6	6	13	9	5
243.293607	-0.000003	0.2E-03	15	13	2	16	14	3
243.444588	-0.000042	0.2E-03	11	8	4	12	11	1
245.919927	-0.000073	0.2E-03	15	15	0	16	16	1
246.977555	-0.000058	0.2E-03	15	14	1	16	15	2
247.167531	-0.000066	0.2E-03	15	13	3	16	14	2
247.544345	-0.000135	0.2E-03	15	14	2	16	15	1
253.337856	0.000288	0.2E-03	14	10	5	15	11	4
255.134236	0.000053	0.2E-03	13	8	6	14	9	5
255.454760	-0.000043	0.2E-03	17	13	4	18	14	5

TABLE II—*Continued*

Obs. Freq.	Obs.-Calc.	Unc.	J Ka Kc lower	J Ka Kc upper	Obs. Freq.	Obs.-Calc.	Unc.	J Ka Kc lower	J Ka Kc upper
257.297161	-0.000112	0.2E-03	13 7 6	14 10 5	294.118147	-0.000654	0.2E-03	12 7 6	13 10 3
257.415813	-0.000178	0.2E-03	11 7 5	12 10 2	294.176781	-0.000137	0.2E-03	14 11 4	15 14 1
258.271168	0.000035	0.2E-03	16 14 2	17 15 3	294.272928	-0.000145	0.2E-03	18 14 5	19 15 4
259.876303	-0.000091	0.2E-03	16 16 0	17 17 1	296.186852	0.000053	0.2E-03	14 6 9	15 7 8
259.940391	0.000074	0.2E-03	16 16 1	17 17 0	296.196407	0.000118	0.2E-03	14 5 9	15 8 8
259.995312	-0.000036	0.2E-03	12 5 8	13 6 7	296.209926	0.000164	0.2E-03	12 1 12	13 2 11
260.007893	0.000028	0.2E-03	12 4 8	13 7 7	296.209926	0.000163	0.2E-03	12 0 12	13 3 11
260.627268	-0.000032	0.2E-03	13 10 3	14 13 2	299.924132	-0.000140	0.2E-03	19 17 2	20 18 3
260.801312	-0.000065	0.2E-03	16 14 3	17 15 2	300.421235	-0.000169	0.2E-03	14 10 5	15 13 2
261.453045	-0.000059	0.2E-03	16 15 1	17 16 2	300.577843	0.000031	0.2E-03	13 2 11	14 5 10
261.822915	-0.000113	0.2E-03	16 15 2	17 16 1	300.577843	0.000041	0.2E-03	13 3 11	14 4 10
262.213714	-0.000060	0.2E-03	13 11 2	14 14 1	300.612073	0.000166	0.2E-03	15 8 8	16 9 7
263.616842	-0.000126	0.2E-03	11 1 10	12 4 9	300.838795	-0.000043	0.2E-03	15 7 8	16 10 7
263.616842	-0.000117	0.2E-03	11 2 10	12 3 9	303.680499	0.000098	0.2E-03	19 18 1	20 19 2
263.756719	0.000079	0.2E-03	15 11 5	16 12 4	305.052044	0.000271	0.2E-03	14 5 10	15 6 9
263.793099	-0.000070	0.2E-03	16 13 4	17 14 3	305.052044	-0.000480	0.2E+13	14 4 10	15 7 9
264.973469	0.000047	0.2E-03	13 7 7	14 8 6	306.010641	0.000035	0.2E-03	16 9 7	17 12 6
265.299971	-0.000038	0.2E-03	13 6 7	14 9 6	307.810620	0.000028	0.2E-03	18 13 6	19 14 5
267.493033	0.000122	0.2E-03	14 9 6	15 10 5	309.496470	0.000040	0.2E-03	15 7 9	16 8 8
267.545426	-0.000078	0.2E-03	14 9 5	15 12 4	309.523320	-0.000026	0.2E-03	15 6 9	16 9 8
267.826493	0.000621	0.2E-03	17 14 3	18 15 4	309.916710	-0.000145	0.2E-03	13 1 12	14 4 11
271.195524	-0.000042	0.2E-03	12 8 5	13 11 2	309.916710	-0.000145	0.2E-03	13 2 12	14 3 11
271.498773	-0.000201	0.2E-03	14 8 6	15 11 5	313.441955	0.000002	0.2E-03	16 9 8	17 10 7
272.686521	0.000139	0.2E-03	17 15 2	18 16 3	313.954141	0.000014	0.2E-03	16 8 8	17 11 7
272.795986	0.000049	0.2E-03	11 0 11	12 3 10	314.092724	0.000229	0.2E-03	14 4 11	15 5 10
272.795986	0.000049	0.2E-03	11 1 11	12 2 10	314.092724	0.000181	0.2E-03	14 3 11	15 6 10
273.722427	-0.000081	0.2E-03	17 17 0	18 18 1	315.997886	-0.000284	0.2E-03	17 11 6	18 14 5
273.835646	0.000035	0.2E-03	13 6 8	14 7 7	318.353755	0.000070	0.2E-03	15 5 10	16 8 9
273.848576	0.000031	0.2E-03	16 12 5	17 13 4	318.353755	0.002597	0.2E+13	15 6 10	16 7 9
273.871457	-0.000022	0.2E-03	13 5 8	14 8 7	319.534593	0.000243	0.2E-03	17 10 7	18 13 6
274.318169	0.000129	0.2E-03	17 15 3	18 16 2	319.559488	0.000094	0.2E-03	13 0 13	14 3 12
275.713787	-0.000091	0.2E-03	17 16 1	18 17 2	319.559488	0.000094	0.2E-03	13 1 13	14 2 12
275.955754	-0.000108	0.2E-03	17 16 2	18 17 1	322.508142	-0.000131	0.2E-03	16 8 9	17 9 8
276.243271	0.000155	0.2E-03	17 14 4	18 15 3	322.578319	-0.000336	0.2E-03	16 7 9	17 10 8
277.082043	0.000122	0.2E-03	13 10 4	14 13 1	323.368749	0.000032	0.2E-03	14 3 12	15 4 11
277.676156	-0.000014	0.2E-03	12 3 10	13 4 9	323.368749	0.000030	0.2E-03	14 2 12	15 5 11
277.676156	-0.000060	0.2E-03	12 2 10	13 5 9	326.860875	0.000279	0.2E-03	17 9 8	18 12 7
278.277965	-0.000180	0.2E-03	14 8 7	15 9 6	327.348878	0.000059	0.2E-03	15 4 11	16 7 10
278.939992	0.000261	0.2E-03	15 10 6	16 11 5	327.348878	0.000251	0.2E+13	15 5 11	16 6 10
279.000541	-0.000034	0.2E-03	14 7 7	15 10 6	331.377649	-0.000277	0.2E-03	16 7 10	17 8 9
280.957771	0.000121	0.2E-03	14 11 3	15 14 2	331.385308	-0.000322	0.2E-03	16 6 10	17 9 9
282.602194	0.000311	0.2E-03	13 5 9	14 6 8	332.932922	-0.000253	0.2E-03	14 2 13	15 3 12
282.604923	-0.000004	0.2E-03	13 4 9	14 7 8	332.932922	-0.000253	0.2E-03	14 1 13	15 4 12
283.922298	-0.000070	0.2E-03	17 13 5	18 14 4	335.359114	-0.000247	0.2E-03	17 8 9	18 11 8
284.195478	-0.000149	0.2E-03	15 10 5	16 13 4	336.561962	0.000210	0.2E-03	15 3 12	16 6 11
285.528626	-0.000092	0.2E-03	13 9 5	14 12 2	336.561962	0.000221	0.2E-03	15 4 12	16 5 11
285.867965	-0.000332	0.2E-03	15 9 6	16 12 5	340.339826	0.000110	0.2E-03	16 6 11	17 7 10
286.563823	0.000119	0.2E-03	18 16 2	19 17 3	340.339826	-0.000581	0.2E+13	16 5 11	17 8 10
286.810265	-0.000132	0.2E-03	12 2 11	13 3 10	342.842111	0.000123	0.2E-03	14 1 14	15 2 13
286.810265	-0.000134	0.2E-03	12 1 11	13 4 10	342.842111	0.000123	0.2E-03	14 0 14	15 3 13
287.388145	0.000047	0.2E-03	14 7 8	15 8 7	344.117778	-0.000351	0.2E-03	17 8 10	18 9 9
287.482007	0.000082	0.2E-03	14 6 8	15 9 7	344.139154	-0.000574	0.2E-03	17 7 10	18 10 9
287.511010	-0.000186	0.2E-03	18 18 0	19 19 1	346.045678	-0.000033	0.2E-03	15 2 13	16 5 12
287.610415	0.000008	0.2E-03	18 16 3	19 17 2	346.045678	-0.000032	0.2E-03	15 3 13	16 4 12
288.995819	0.000716	0.2E-03	18 15 4	19 16 3	349.492202	0.000174	0.2E-03	16 5 12	17 6 11
289.399339	0.000443	0.2E-03	16 11 6	17 12 5	349.492202	0.000124	0.2E-03	16 4 12	17 7 11
289.783199	0.000041	0.2E-03	18 17 1	19 18 2	353.059727	-0.000640	0.2E-03	17 6 11	18 9 10
289.941660	-0.000196	0.2E-03	18 17 2	19 18 1	353.059727	0.001608	0.2E+13	17 7 11	18 8 10
290.377390	-0.000056	0.2E-03	15 11 4	16 14 3	355.855414	-0.000560	0.2E-03	15 1 14	16 4 13
291.051092	0.000044	0.2E-03	15 9 7	16 10 6	355.855414	-0.000560	0.2E-03	15 2 14	16 3 13
291.490695	0.000030	0.2E-03	13 3 10	14 6 9	358.896126	0.000787	0.2E-03	16 4 13	17 5 12
291.490695	0.000229	0.2E+13	13 4 10	14 5 9	358.896126	0.000784	0.2E-03	16 3 13	17 6 12
292.543246	-0.000076	0.2E-03	15 8 7	16 11 6					

$$|1'\rangle = \frac{1}{2}(|1\rangle + |2\rangle + |3\rangle + |4\rangle)$$

$$|2'\rangle = \frac{1}{2}(|1\rangle - |2\rangle + |3\rangle - |4\rangle)$$

$$|3'\rangle = \frac{1}{2}(|1\rangle + |2\rangle - |3\rangle - |4\rangle)$$

$$|4'\rangle = \frac{1}{2}(|1\rangle - |2\rangle - |3\rangle + |4\rangle). \qquad (6)$$

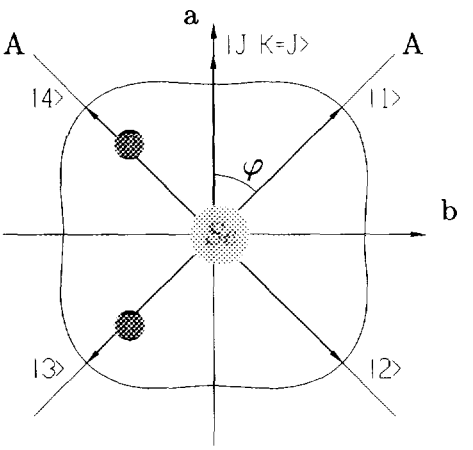

FIG. 2. The H_2Se body-frame, the cross-section of the RES with the *ab*-plane, new precession axes A, and the localized rotational states shown as vectors.

each transform according to one of the irreducible representations of the D_2 group and we can determine the correlation to the true eigenfunctions $\Psi_{J_{J0}}$, $\Psi_{J_{J1}}$, $\Psi_{J_{J-1,1}}$, and $\Psi_{J_{J-1,2}}$ from Table 11-2 of Ref. (*15*). We expect that for increasing J, the wavefunctions of Eq. (6) also become increasingly better approximations of the eigenfunctions for the Hamiltonian in Eq. (1). If we assume that the wavefunctions of Eq. (6) are indeed the exact eigenfunctions $\Psi_{J_{J0}}$, $\Psi_{J_{J1}}$, $\Psi_{J_{J-1,1}}$, and $\Psi_{J_{J-1,2}}$ of the Hamiltonian, we can determine the localization angle φ by subjecting these functions to transformations inverse to those given in Eqs. (2)–(5). For example, we can invert Eq. (6) to determine the wavefunction $|1\rangle$, and we can then subject this function to the rotation $R_C^{-\varphi}$ (the inverse of the transformation in Eq. (2)):

$$\varphi\colon R_C^{-\varphi}\tfrac{1}{2}(\Psi_{J_{J0}} + \Psi_{J_{J1}} + \Psi_{J_{J-1,1}} + \Psi_{J_{J-1,2}}) = \sum a_K|JK\rangle \simeq |JJ\rangle. \qquad (7)$$

We write the resulting rotated function as a linear combination $\sum a_K|JK\rangle$ of symmetric-top basis functions, and this function will have its maximum contribution from the $|JJ\rangle$ function so that a_J will be the numerically largest expansion coefficient. In Fig. 3b we show the expansion coefficients a_K resulting from such transformations carried out for $J = 23$. As expected, the resulting a_K-distribution becomes more sharp as J increases (Fig. 3c). For a given J-value, we can determine φ as the angle that leads to maximum a_J in Eq. (7), and the φ-values obtained in this way are shown as squares in Fig. 4. By comparison of this figure and Fig. 5 of Ref. (*1*), where the dependence of the angular position of the "newborn" RES maximum on J was presented, it is evident that both pictures give nearly the same dependence when J is higher than 15. We observe again that the angle approaches a constant value with increasing J. If we try to make a similar manipulation with the corresponding rigid rotor eigenfunctions the result will be drastically different (Fig. 4, triangles). The difference would be even more transparent if the rigid rotor corresponding to the H_2Se molecule were not so close to a symmetric rotor.

The equations (2)–(6) also make it possible to calculate the linestrengths for transitions between localized states. If we take into account that the overlapping of wave-

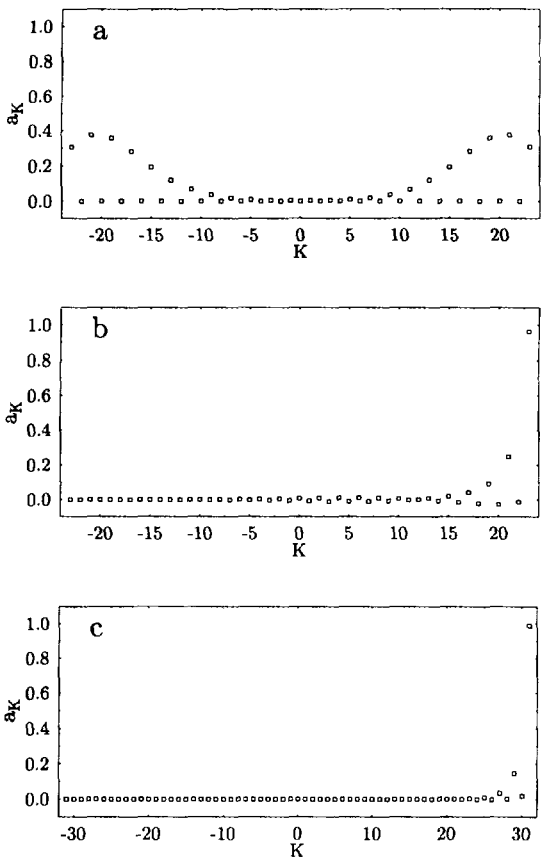

FIG. 3. (a) a_K-expansion coefficients of the $23_{23\,0}$ rotational state of $H_2{}^{80}Se$ in the $|JK\rangle$ symmetric-top basis set; (b) a_K-expansion coefficients as a result of the back transformation according to Eq. (7) with $\varphi = 34°$ for $J = 23$; (c) the same as (b), but with $\varphi = 38°$ for $J = 31$.

functions, introduced in Eqs. (2)–(5), becomes negligible with increasing J, we can easily obtain the very simple results

$$\text{Linestrengths} \begin{pmatrix} J_{J-1,1} \rightarrow J_{J0} \\ J_{J-1,2} \rightarrow J_{J1} \end{pmatrix} \simeq 2 \sin^2\varphi(J + 1/2) \tag{8}$$

$$\text{Linestrengths} \begin{pmatrix} J_{J0} \rightarrow J + 1_{J+1,1} \\ J_{J1} \rightarrow J + 1_{J+1,0} \\ J_{J-1,1} \rightarrow J + 1_{J2} \\ J_{J-1,2} \rightarrow J + 1_{J1} \end{pmatrix} \simeq \cos^2\varphi(J + 1/2). \tag{9}$$

However the dependence on J is not so simple as one would expect from Eqs. (8) and (9) because φ is also a function of J. If we assume φ to be constant, which is approximately true for very high J, we will get a simple linear dependence. It is interesting to note here that if $\varphi = 45°$ the line strengths of Eqs. (8) and (9) will be very close to the linestrengths of the transitions $J_{J-1,1} \rightarrow J_{J0}$ and $J_{J1} \rightarrow J + 1_{J+1,0}$ of a symmetric rotor. These linestrengths are equal to $J + \frac{1}{2}$ and $J/2$, respectively.

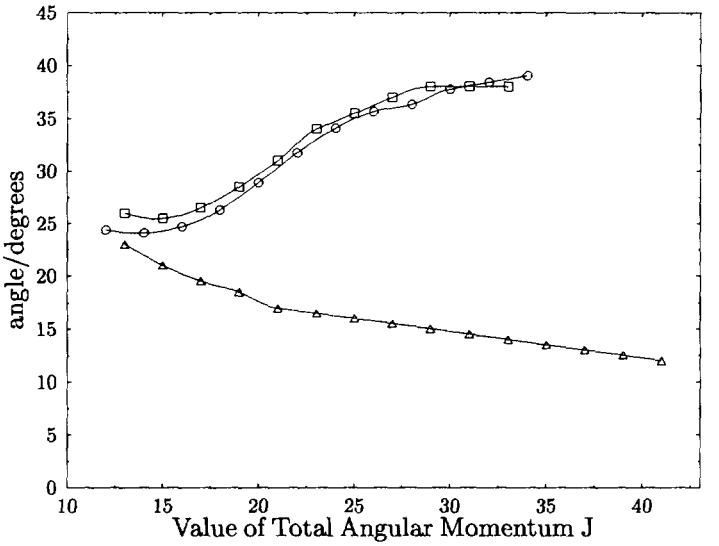

FIG. 4. The calculation of the localization angle φ: (1) according to Eq. (7) for H_2Se (squares) and rigid rotor (triangles); (2) using Eqs. (8) and (9) together with calculations of the H_2Se linestrengths (circles). For further comments, see the text.

Equation (9) supports the fact that no strong perturbation of the corresponding linestrengths was observed in the FIR spectrum. Equation (8) can be applied to the MW transitions of Ref. (*1–3*) and explains the strong linestrength distortions observed there. On the other hand Eqs. (8) and (9) again gives us the possibility of calculating the localization angle if we obtain the linestrengths directly from the rotational Hamiltonian of Eq. (1). The results of such calculations are shown in Fig. 4 as circles and are in a good agreement with all earlier estimations.

CONCLUSION

The analysis of the extensive experimental data recorded in the present work has allowed a further characterization of the fourfold clustering effect exhibited by the rotational energy levels superimposed on the vibrational ground state of the H_2Se molecule. We have shown that in agreement with the RES analysis of Ref. (*1*), the fourfold cluster states are strongly localized around new precession axes. The localization of rotational states causes both the fourfold clustering of the rotational energies and the observed linestrength distortions, and so these two anomalies have a common origin. The localization of n-fold cluster wavefunctions around $n/2$ precession axes is not limited to H_2Se but is also observed, for example, in spherical-top molecules. The very recent analysis by Larsen and Brodersen (*16*) of calculated rotation–vibration eigenfunctions for CF_4 provides an excellent example of such studies.

ACKNOWLEDGMENTS

We thank B. P. Winnewisser and M. Winnewisser for useful discussions and for critically reading the manuscript. The work of I.N.K., S.K., and P.J. was supported by the Deutsche Forschungsgemeinschaft and by the Fonds der Chemischen Industrie. P.J. acknowledges further support from the Dr. Otto Röhm Gedächtnisstiftung and from the Fritz Thyssen-Stiftung. We thank J.-M. Flaud for pointing out a mistake in an earlier version of this paper.

RECEIVED: September 11, 1992

REFERENCES

1. I. N. KOZIN, S. P. BELOV, O. L. POLYANSKY, AND M. YU. TRETYAKOV, *J. Mol. Spectrosc.* **152,** 13–28 (1992).
2. M. YU. TRETYAKOV, S. P. BELOV, I. N. KOZIN, AND O. L. POLYANSKY, *J. Mol. Spectrosc.* **154,** 163–168 (1992).
3. I. N. KOZIN, O. L. POLYANSKY, S. I. PRIPOLZIN, AND V. L. VAKS, *J. Mol. Spectrosc.* **156,** 504–506 (1992).
4. E. D. PALIK AND R. A. OETJEN, *J. Mol. Spectrosc.* **1,** 223–238 (1957).
5. G. GUELACHVILI AND K. NARAHARI RAO, "Handbook of Infrared Standards," Academic Press, Orlando, Florida, 1986.
6. A. W. JACHE, P. W. MOSER AND W. GORDY, *J. Chem. Phys.* **25,** 209–210 (1956).
7. P. HELMINGER AND F. C. DE LUCIA, *J. Mol. Spectrosc.* **58,** 375–383 (1975).
8. J. R. GILLIS AND T. H. EDWARDS, *J. Mol. Spectrosc.* **85,** 74–84 (1981).
9. WM. C. LANE, T. H. EDWARDS, J. R. GILLIS, F. S. BONOMO, AND F. J. MURCRAY, *J. Mol. Spectrosc.* **107,** 306–317 (1984).
10. B. P. WINNEWISSER, *The Analyst* **117,** 343–349 (1992).
11. B. I. ZHILINSKII AND I. M. PAVLICHENKOV, *Opt. Spectrosc. (USSR)* **64,** 688–690 (1988). [In Russian]
12. J. MAKAREWICZ AND J. PYKA, *Mol. Phys.* **69,** 107–127 (1989).
13. W. G. HARTER AND C. W. PATTERSON, *J. Chem. Phys.* **80,** 4241–4261 (1984).
14. I. M. PAVLICHENKOV AND B. I. ZHILINSKII, *Ann. Phys. (N.Y.)* **184,** 1–32 (1988).
15. P. R. BUNKER, "Molecular Symmetry and Spectroscopy," Academic Press, London, 1979.
16. S. G. LARSEN AND S. BRODERSEN, submitted for publication.